

Enhanced Loss of Fast Ions During Mode Conversion Ion Bernstein Wave Heating in TFTR

D. S. Darrow, R. Majeski, N. J. Fisch, R. F. Heeter, H. W. Herrmann, M. C. Herrmann, M. C. Zarnstorff, and S. J. Zweben

Princeton University, Plasma Physics Laboratory,
PO Box 451, Princeton, New Jersey 08543-0451, USA

RECEIVED
MAR 13 1996
OSTI

Abstract

A strong interaction of fast ions with ion Bernstein waves has been observed in TFTR. It results in a large increase in the fast ion loss rate, and heats the lost particles to several MeV. The lost ions are observed at the passing/trapped boundary and appear to be either DD fusion produced tritons or accelerated D neutral beam ions. Under some conditions, enhanced loss of DT alpha particles is also seen. The losses provide experimental support for some of the elements required for alpha energy channeling.

Knowledge of the alpha particle behavior in a tokamak fusion reactor will be essential to its successful operation. For instance, although energetic alpha particles make up only ~0.6% of the total particle density in the Tokamak Fusion Test Reactor (TFTR), they comprise up to 10% of the central energy density. The alphas therefore provide a possible source of free energy for instabilities in the plasma.¹ The energy in the alphas also could damage the first wall of a reactor if it is deposited on the wall in large amounts or in a strongly localized manner.² In a more beneficial vein, it has been suggested that the alpha energy could be transferred via plasma waves to heat the fuel ions directly or to drive the plasma current.^{3,4} To achieve this latter goal, it is necessary to understand the interaction of fusion products with plasma waves.

This letter reports observations of strongly enhanced losses of fast ions from TFTR plasmas heated by ion Bernstein waves (IBWs)⁵. The losses are many times the usual first orbit losses of charged fusion products (CFPs) and have characteristics unlike any seen previously in TFTR. Information concerning the losses is of interest because it illuminates the physics of the interactions between the IBWs and the fast ions.

In TFTR, IBWs are generated by mode conversion, at the two ion hybrid layer, of fast waves in the ion cyclotron range of frequencies (ICRF) launched by external antennas at the outboard midplane of the tokamak.⁶ The resulting IBW is absorbed ~70% by electrons within a few cm of the mode conversion layer. The position of the layer can be controlled by varying the toroidal field strength and the fractional abundance of ³He (the remainder of the plasma being principally D and ⁴He).

Typical discharge conditions for IBW experiments in TFTR are: $R=2.625$ m, $a=0.99$ m, $B_T=4.8$ T, $I_p=1.4$ MA, $n_e(0)=5 \times 10^{19}$ m⁻³, $n_{3He}/n_e \geq 0.15$, $T_e(0)=7$ keV, $P_{NB}=0-10$ MW, and $P_{RF}=3-5$ MW (43 MHz). The fast ion loss rate is measured by detectors at 90°, 60°, 45°, and 20° below the outer midplane, at a single toroidal location.⁷ The detectors are unable to discriminate between ions of different charge or mass and are insensitive to hydrogenic ions with $E < 400$ keV.

Figure 1 compares the time histories of two IBW discharges which differ only in the fraction of ³He present. The broken line shows the data from a plasma with $n_{3He}/n_e=0.15$ while the solid line shows the signals for one with $n_{3He}/n_e=0.20$. The ICRF and neutral beam (NB) powers are very similar for the two discharges, as are the neutron rates. The total fast ion loss rate for the $n_{3He}/n_e=0.20$ case exceeds that in the other on all detectors by up to a factor of 10. The losses in the $n_{3He}/n_e=0.15$ plasma, except in the 45° detector, are about at the level of first orbit loss for CFPs (an irreducible loss due to fat banana orbits which intersect the wall), amounting to ~10% of the CFP birth rate.⁹ In contrast, losses of CFPs during ICRF fast wave heating have been, at most, a factor of 1.8 above first orbit loss at comparable powers.⁸ The sometimes sudden variation of the losses shown in Fig. 1 appears to be correlated with small changes in n_e .

Another comparison shot, identical to those shown in Fig. 1 but with no NB injection and therefore negligible fusion rate, has no detectable losses. This implies that the lost ions are either CFPs or NB ions accelerated by the IBW. An energetic ³He ion tail is discounted as a possible source of the loss due to the high concentration of ³He and the observed correlation of the loss only with NB injection.

Figure 2 compares the gyroradius distribution of the loss in the 90° detector during IBWH to first orbit loss of CFPs. In this case, the first orbit loss distribution shows the effect of instrumental broadening, since first orbit loss consists of birth-energy CFPs exclusively. The distribution during IBWH peaks at a higher gyroradius and has a larger full width at half maximum than does the first orbit loss distribution. Both of these signatures indicate that the escaping particles have been heated significantly above the CFP birth energies.

Numerically modeled distributions of monoenergetic particle loss are most similar to the observations for the case of a CFP at 50% above its birth energy. If the escaping particles are CFPs, they are thought (see below) to be principally DD fusion tritons born at 1 MeV, in which case the IBW is typically adding 500 keV to the energy of each escaping particle. If the lost particles are accelerated NB ions, they are at ~2 MeV, indicating an even larger heating than that inferred for the CFPs. However, the creation of a fast tail of beam ions should result in a substantial flux of ions well below the energy of fusion products, something not seen in the gyroradius measurements. Combining the gyroradius information with the time history shown in Fig. 1 yields a rate of diffusion in energy of these lost ions of ~1.6 MeV²/sec if they are tritons and ~25 MeV²/sec if they are NB ions. The lost ions appear at the pitch angle of the passing/trapped boundary, meaning that the IBW transports them outward in minor radius, gives them additional v_{\perp} , or both.

Fusion products result chiefly from DD and D³He beam-plasma reactions, at production rates which are of the same order of magnitude. Lacking a measurement of the lost ion charge or mass, it is impossible to ascertain exactly which fast ions are expelled. However, various direct and indirect arguments too lengthy to present here point, if the loss is of CFPs at all, to the 1 MeV DD triton. If the D beams are replaced with T beams, the IBW-related loss appears to vanish. This is consistent with the lost ions being either fusion tritons or accelerated D beam ions, since the source for both has been removed in changing to T beams.

DISCLAIMER

**Portions of this document may be illegible
in electronic image products. Images are
produced from the best available original
document.**

Figure 3 shows the time history of the neutron rate and loss rate to the 60° detector in an experiment with short NB injection during IBWH. The dashed line in the neutron rate plot indicates the neutron production in a shot without rf. Losses in the 60° detector rise sharply ~100 ms after the beam pulse ends, and remain at many times the expected CFP first orbit loss level until the IBW pulse ends. The loss to the other probes is similar. In this discharge, the total time-integral of the loss, assuming a poloidal angular distribution like that of first orbit loss, is more than the total CFP production in the plasma as determined by integrating the neutron rate. This seems most easily explained if the lost particles are accelerated beam ions, since the beam ion density is $\sim 10^4$ times larger than the CFP density. An IBW-produced D tail could also explain the larger and longer-lasting neutron signal which is seen when the IBW is present. However, a tail should result in some signature of anisotropy in the magnetic measurements of the plasma's stored energy, and that is not observed. Alternatively, these losses may be of D^3He fusion products, whose source rate is not measured in the neutron signal.

Figure 4 shows the loss rate at the 90° detector as a function of B_T . The loss is maximum just below 5.0 T, and falls to background levels within a 5% change in field in either direction. By scanning B_T , the IBW layer position is scanned in major radius. The maximum loss occurs when the IBW layer lies on the magnetic axis. A similar response is also seen when the IBW layer position is moved by varying n_{3He} while holding B_T fixed. In contrast, losses of CFPs during ICRF fast wave heating show a significantly broader dependence on B_T , and do not depend on plasma composition. Hence, Fig. 4 confirms that the IBW is the cause of the enhanced losses seen.

When T is puffed into plasmas with $B_T=5.3$ T and $n_e(0)=8 \times 10^{19} \text{ m}^{-3}$, apparent losses of alpha particles result. Fig. 5 compares similar discharges made with and without T puffs. Both signals show the characteristics of IBW enhancement above first orbit loss but, during T puffing, the fluxes to the 60° and 45° escaping ion detectors increase by about a factor of five. This enhancement suggests that DT alpha particles are being lost, since the T puff is only a minor perturbation to the plasma parameters except for the alphas it produces. The gyroradius of the particles lost to the 60° detector under these conditions is consistent with birth energy alphas. Both these results are naturally explained if it is CFPs which are being lost, but harder to explain if accelerated NB ions are being lost.

The TFTR ICRF antennas allow directional launch of the fast waves, which results in directional propagation of the IBWs. For the data described so far, nondirectional phasing was used, resulting in equal amplitude waves in the co- and counter- I_p directions. When the antennas are phased to launch waves propagating in the co- I_p direction, no enhanced losses are observed. The losses *are* seen, however, with counter- I_p traveling waves, and they occur at power levels lower than those needed with 180° phasing.

To understand how the IBW causes fast ions to be lost from the plasma, we have simulated particle orbits under interaction with the mode converted IBW.¹¹ In this simulation, a single fast ion orbit is followed. The mode converted wave is assumed to exist in a slab near the center of the plasma 15 cm wide and extending from the top to the bottom of the plasma. If the particle passes through this slab and is resonant with the IBW, a random change in the particle's energy is made. Upon repeated interaction with the wave, the resonant particle diffuses. In this model, there is no collisional diffusion.

The effect of diffusion on a typical countergoing fusion-produced triton is simulated in Fig. 6. Here the launched fast wave propagates counter to the plasma current. The figure depicts, for the initial conditions used, possible ranges of orbits of the triton as it exchanges energy with the IBW. If, upon diffusing in the wave, the triton eventually leaves the plasma, it must do so as shown: namely by first gaining 0.5 MeV, crossing the passing/trapped boundary, and striking the wall at about 90° below the midplane. A similar behavior is seen in modeling D beam ion orbits. The results for this typical orbit are in close agreement with the experimental observations. This agreement supports details of the wave propagation itself,^{10,11} which are utilized in the modeling. The theoretical calculations that lead to this model also predict cooling of alpha particles when multiple waves are present.¹²

Alpha energy channeling requires extraction of energy from the alphas by the wave, ion heating or current drive by the wave, and removal of the cooled alphas from the plasma. The result reported here, of a fast ion diffusion rate in energy greater than 1 MeV²/sec, is sufficient that the wave can extract energy from the alphas significantly more rapidly than collisions can. This observation and the success of the theoretical model in simulating the TFTR results lends support to the hope that the IBW can be an important component of an alpha energy channeling scenario.

This work supported by US DoE contract DE-AC02-76-CHO-3073. Two authors (MCH & RFH) acknowledge the support of the Fannie and John Hertz Foundation.

References

- ¹C. Z. Cheng, *Phys. Fluids B* **3**, 2463 (1991).
- ²S. Putvinski, et al. in Proc. of the 15th International Conference on Plasma Physics and Controlled Nuclear Fusion Research, Seville, 1994, IAEA-CN-60, paper E-P-4.
- ³N. J. Fisch and J.-M. Rax, *Phys. Rev. Lett.* **69**, 612 (1992).
- ⁴N. J. Fisch, *Phys. Plasmas* **2**, 2375 (1995).
- ⁵I. B. Bernstein, *Phys. Rev.* **109**, 10 (1958).
- ⁶R. Majeski, et al., submitted to *Phys. Rev. Lett.*
- ⁷D. S. Darrow, H. W. Herrmann, D. W. Johnson, R. J. Marsala, R. W. Palladino, and S. J. Zweben, *Rev. Sci. Instrum.* **66**, 476 (1995).
- ⁸D. S. Darrow, S. J. Zweben, R. V. Budny, et al., to appear in *Nucl. Fusion* (1995).
- ⁹R. Boivin, S. J. Zweben, and R. B. White, *Nucl. Fusion* **33**, 449 (1993).
- ¹⁰E. J. Valeo and N. J. Fisch, *Phys. Rev. Lett.* **73**, 3536 (1994).
- ¹¹M. C. Herrmann and N. J. Fisch, 1995 International Sherwood Fusion Theory Conference, Incline Village, NV.
- ¹²N. J. Fisch and M. C. Herrmann, Princeton Plasma Physics Laboratory Report PPPL-3135, to appear in *Nucl. Fusion*, (December 1995).

Figure Captions

Figure 1. ICRF power, NB power, neutron rate, and fast ion loss rate to detectors 90°, 60°, and 45° below the outer midplane for two similar discharges in TFTR. The shot plotted with the dashed line (81548) had $n_{3\text{He}}/n_e=0.15$, while the shot plotted with the solid line (81547) had $n_{3\text{He}}/n_e=0.20$.

Figure 2. Gyroradius distributions of the IBW-related loss (solid line) and first orbit loss of CFPs (dashed line) in the 90° detector. The width of the first orbit loss distribution is due to instrumental broadening, and its peak is at the gyroradius corresponding to birth-energy CFPs. The IBW loss case peaks at a higher gyroradius and is broader, both indicating significant heating of the fast ions before their loss.

Figure 3. NB power, ICRF power, neutron rate, and fast ion loss rate to the 60° detector during a plasma with brief NB injection during the rf pulse. The dashed line in the neutron rate plot indicates the rate measured without rf. The losses seen in other detectors have a time dependence similar to the 60° detector's, rising strongly at ~100 ms after the end of the NB pulse.

Figure 4. Magnitude of the IBW induced loss at the 90° detector versus B_T . Scanning B_T moves the radial location of the IBW layer. The peak of the losses occurs at the point where the IBW layer is on-axis.

Figure 5. Comparison of the ICRF power, neutron rate, and loss rate at the 60° detector for two plasmas, one with T gas puffing and one without. The loss during the shot with T puffing is about five times larger than that in the other shot, suggesting that DT alpha particles are being lost to this detector under these conditions.

Figure 6. Poloidal cross section of orbit of a counter going triton interacting with a mode converted ion Bernstein wave. The magnetic axis is at (1,0).

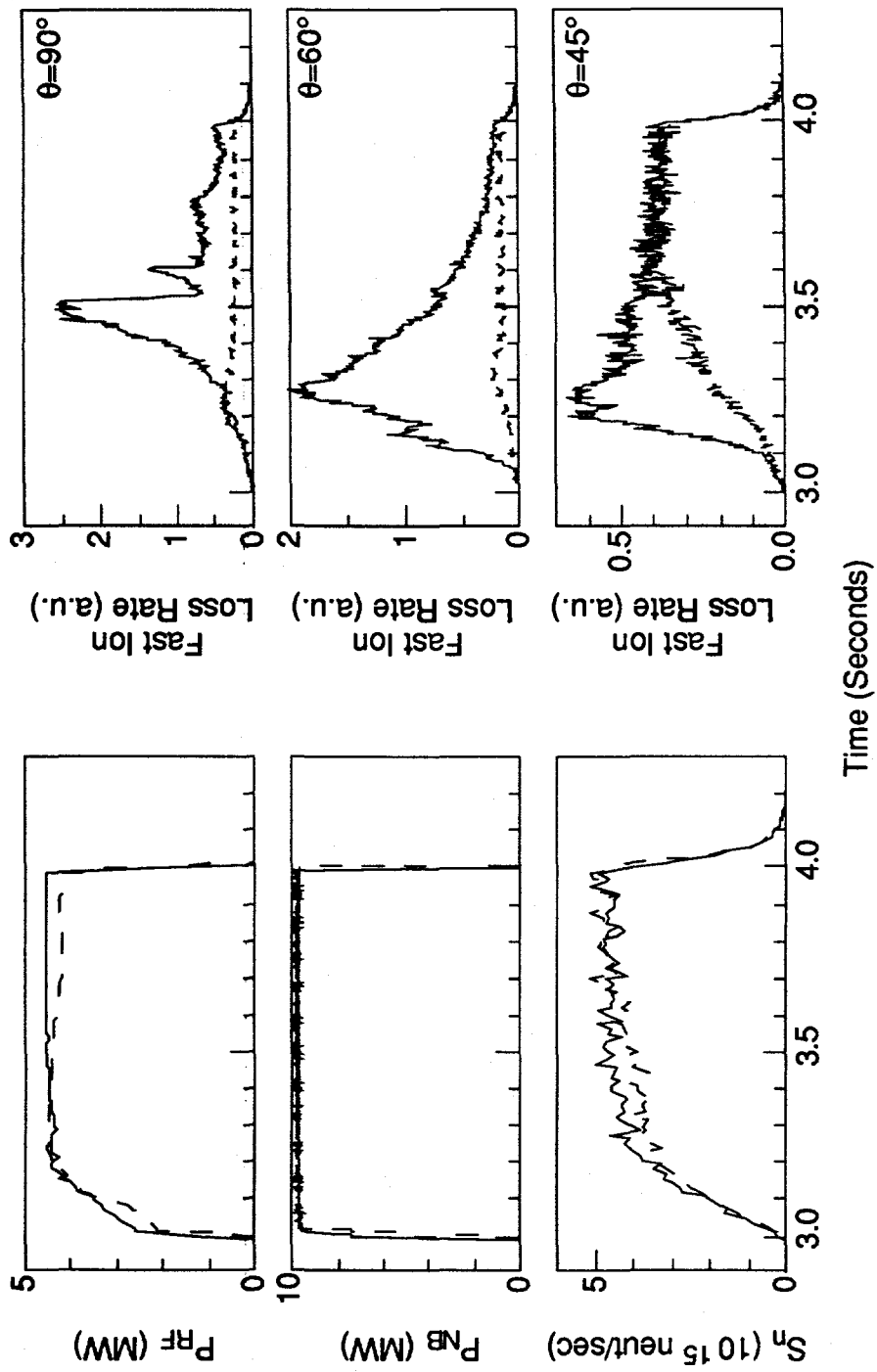


Figure 1

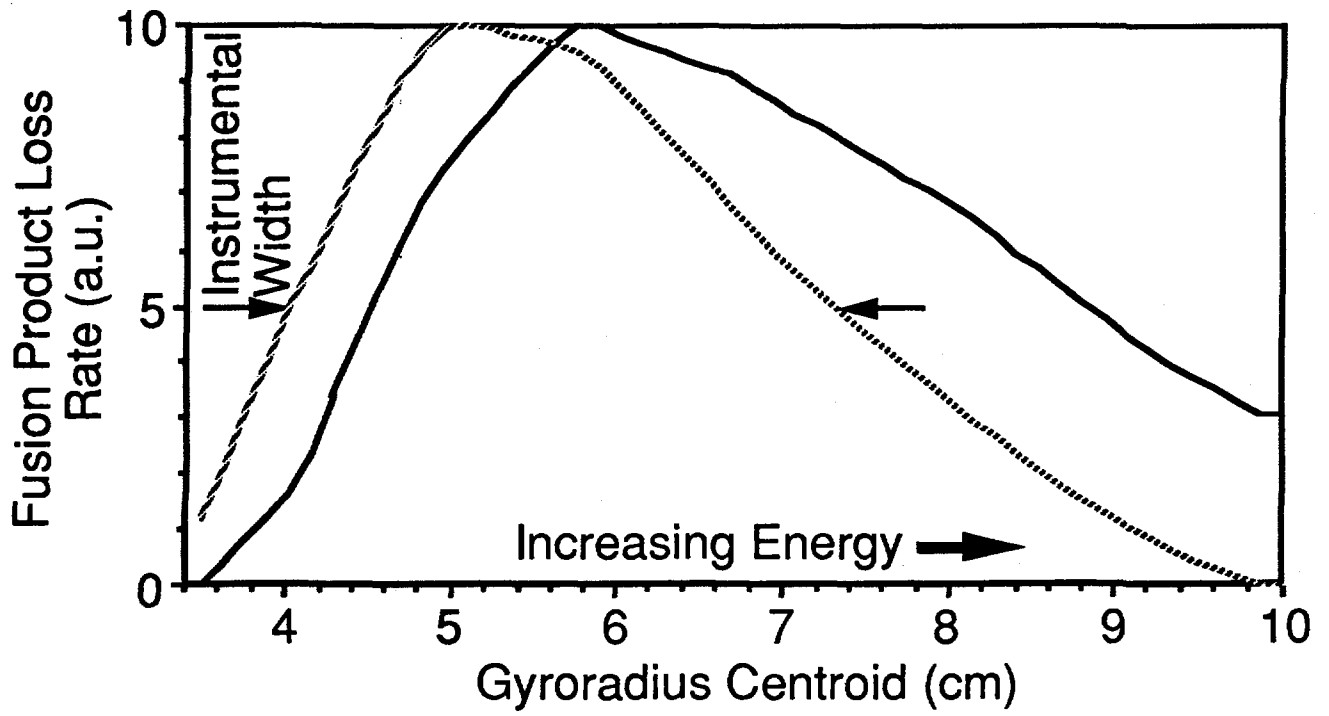


Figure 2

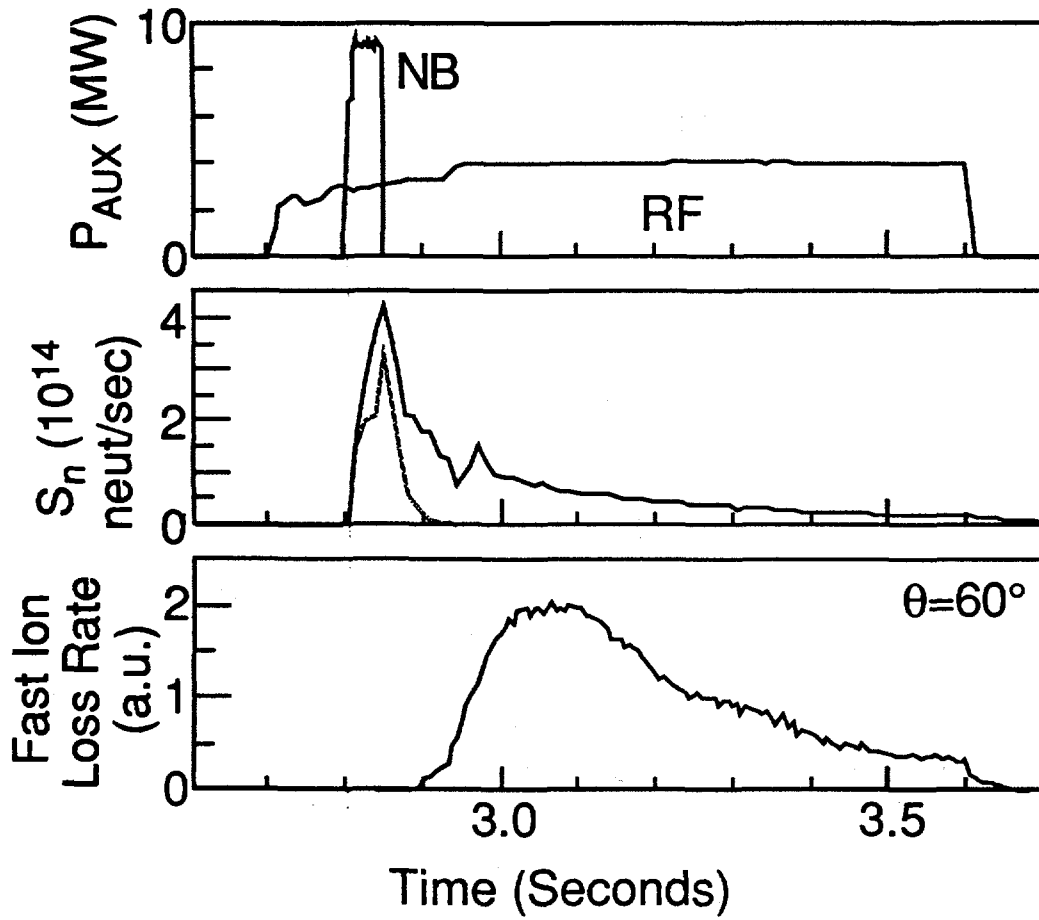


Figure 3

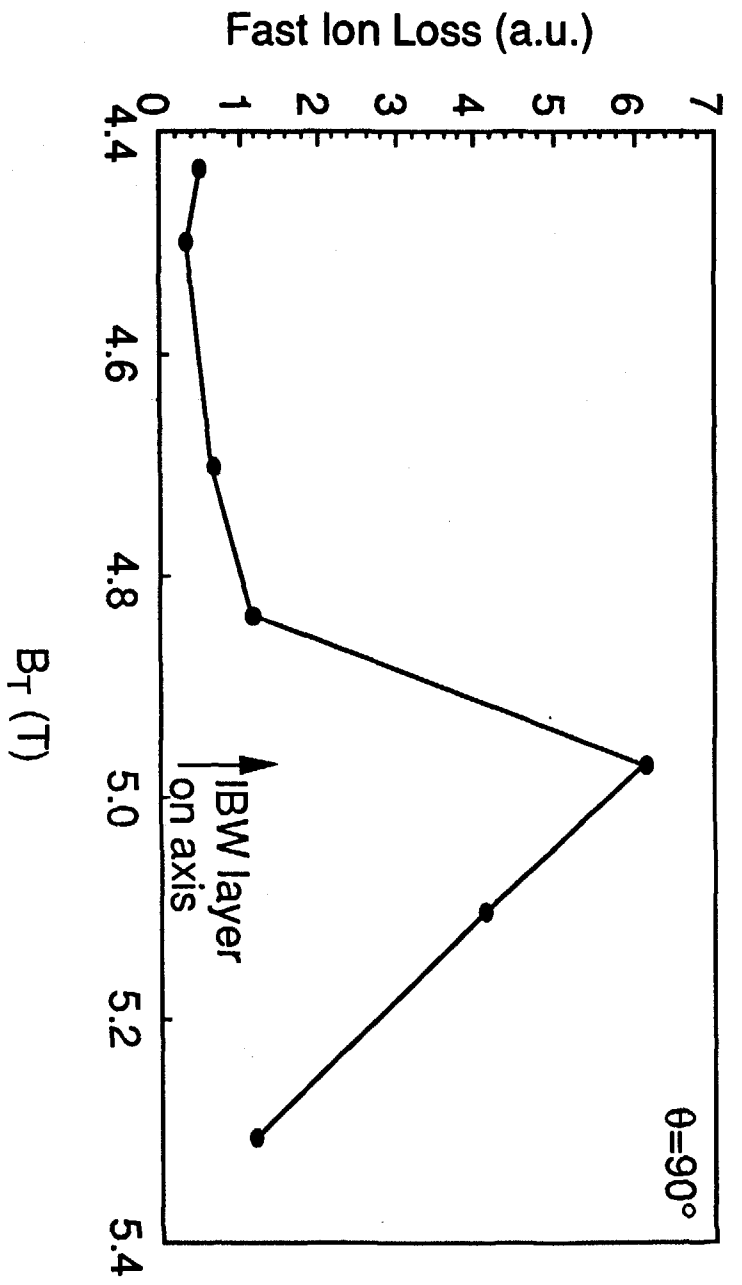


Figure 4

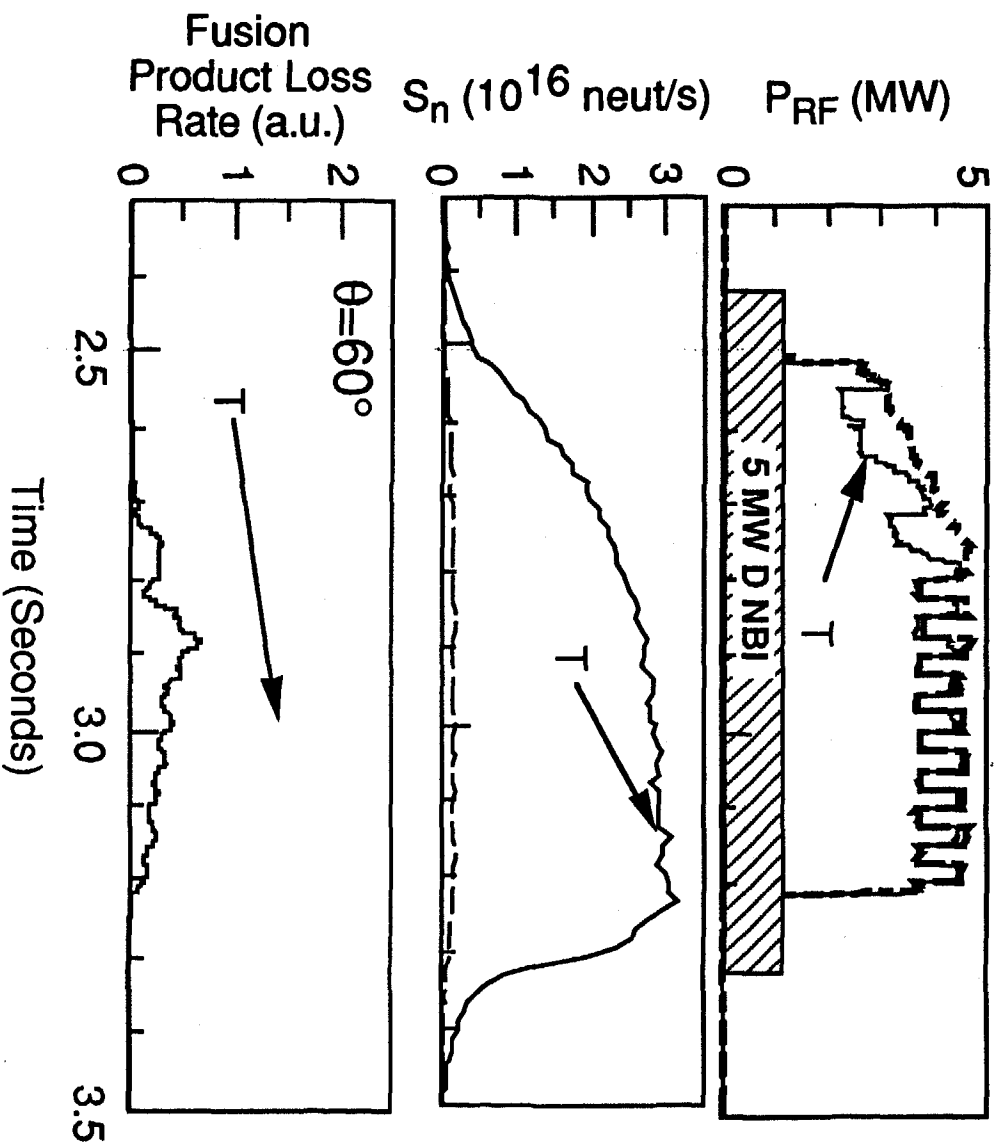
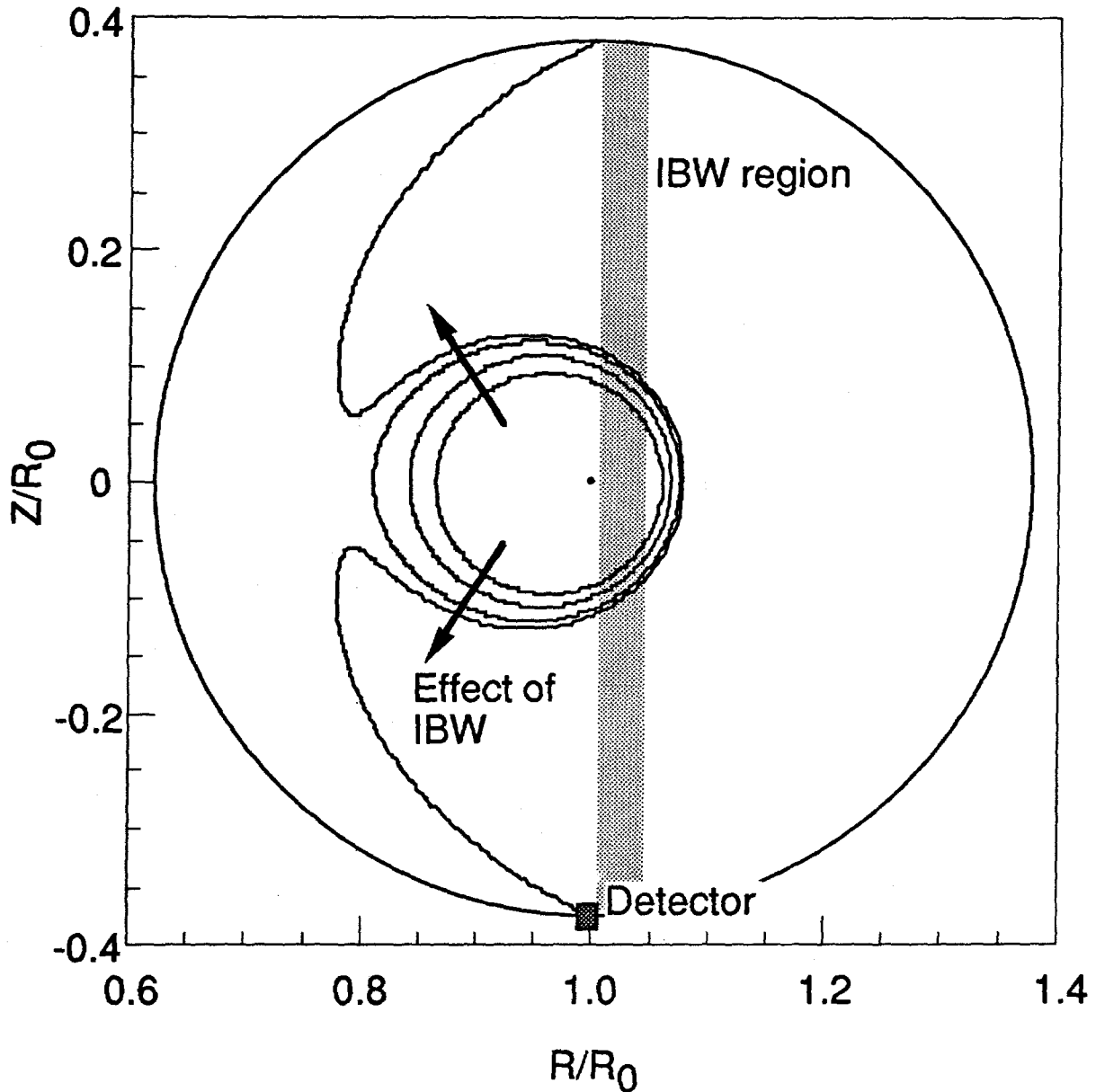


Figure 5



DISCLAIMER

This report was prepared as an account of work sponsored by an agency of the United States Government. Neither the United States Government nor any agency thereof, nor any of their employees, makes any warranty, express or implied, or assumes any legal liability or responsibility for the accuracy, completeness, or usefulness of any information, apparatus, product, or process disclosed, or represents that its use would not infringe privately owned rights. Reference herein to any specific commercial product, process, or service by trade name, trademark, manufacturer, or otherwise does not necessarily constitute or imply its endorsement, recommendation, or favoring by the United States Government or any agency thereof. The views and opinions of authors expressed herein do not necessarily state or reflect those of the United States Government or any agency thereof.

Figure 6

